Robust Performance Control of Electrohydraulic Actuators for Electronic Cam Motion Generation

Dean H. Kim and Tsu-Chin Tsao, *Member, IEEE*

Abstract—**This paper addresses digital control design and implementation for an electrohydraulic servo actuator used in electronic cam motion generation. The actuator dynamics, due to a broad range of motion trajectories, have different degrees of nonlinearity and are represented by a number of linear models with associated bounds of unmodeled dynamics. For each specified range of motion trajectories, a robust performance controller corresponding to the particular linear model is designed to ensure consistent performance under the effect of nonlinear dynamics in the range. Consequently, there is a tradeoff between the robustness and the closed-loop bandwidth. To precisely generate electronic cam motion, a repetitive controller and a feedforward controller are added as plug-ins to the robust performance feedback controller. Experimental results are given to demonstrate the effectiveness of the digital motion control synthesis. Performance of 26-μm maximum tracking error, 6.8-μm root mean square (rms) tracking error, and 4.6-μm rms cycle-to-cycle variations is achieved for tracking a cam profile with 9.4-mm maximum displacement, 1.2-m/s maximum speed, and 1000 m/s^2 maximum acceleration. It is also demonstrated that such performance cannot be achieved if the controller design is based on a small signal model or one with an inadequately small range of motion.**

Index Terms—**Digital control, electrohydraulics, feedforward control, motion control, repetitive control, robust performance, tracking.**

I. Introduction

ELECTRONIC cam motion, where a slave axis driven by an electronically controlled actuator follows a predetermined trajectory as a function of a master axis position, is used in such applications as moving web handling, robotic material handling, and noncircular machining. It has the advantage of software flexibility to quickly change from one cam profile to another, and it eliminates problems associated with the mechanical linkage, such as backlash, friction, engagement de-bouncing, and structural resonance. For the noncircular machining application, the actuator carrying the cutting tool must have large dynamic force capability to generate inertia force for large acceleration (1000 m/s^2) and to compensate for machining force disturbances. Servovalve-driven electrohydraulic actuators are suited for such an application. This paper addresses the motion control of electrohydraulic actuators for cam profile generation.

Exploiting the fact that cam profile tracking in noncircular machining is a control problem of compensating for exogenous periodic signals, Tsao and Tomizuka [1], [2] developed a repetitive control algorithm and implemented it on an electrohydraulic actuator. The controller was designed based on a linear model obtained from small signal perturbations about the null valve and actuator position. The modeling and control method was successful in machining at 600 r/min an elliptical shaped workpiece with 5.0 mm major and minor axis diametrical difference, which corresponds to a periodic reference of 0.31 m/s maximum velocity and 39.4 m/s^2 maximum acceleration. Most other electrohydraulic control literature [3]–[7] also used small signal linear models with various levels of order reduction for applications with less demanding dynamic ranges. In applying noncircular machining to automotive camshaft turning, the class of numerous automotive camshaft lobe profiles in production spans over a much larger motion range in terms of speed, acceleration, and the order of Fourier harmonics required to represent the cam profiles. An example production cam profile that is on the more aggressive side of the class is considered in this paper. The profile has 9.4 mm maximum displacement, about 20 orders of Fourier harmonics, and 1.2 m/s maximum speed and 1000 m/s^2 maximum acceleration, respectively, when it is rotated at 600 r/min. It will be shown that the control design approach based on a small signal model as in [1], [2] is no longer effective in producing precise and consistent cam profile motion.

Hydraulic systems are known to present different levels of nonlinear dynamics according to the range of rated capacity utilized. In particular, a servovalve has substantially different frequency responses as it is excited at different input current magnitudes. An eight-state nonlinear state space model for the servovalve-driven linear displacement actuator was developed in [7] based on first principles. However, it is impractical to attempt to identify the large number of model parameters and preserve the nonlinear model structure because most of the internal state variables are not accessible for measurement. Instead, an appropriate linear representation of the electrohydraulic system with an associated bound on the model mismatch from the actual nonlinear system can be obtained empirically by input–output system identification. This model and its uncertainty bound then can be used for linear controller design.

Given a set of empirical frequency response data corresponding to various levels of input magnitudes, the linear model and its uncertainty bound should be characterized prudently depending on the range of the desired cam profile

Manuscript received May 29, 1997; revised February 11, 1999. Recommended by Associate Editor, H. Jenkins. This work was supported in part by the Motor Vehicle Manufacturing Technology focused area of Advanced Technology Program (ATP MVMT 95-02), National Institute of Standard and Technology.

D. H. Kim is with the Department of Mechanical Engineering, Bradley University, Peoria, IL 61625 USA (e-mail: deankim@bradley.edu).

T.-C. Tsao is with the Mechanical and Aerospace Engineering Department, University of California, Los Angeles CA 90095–1597 USA (e-mail: ttsao@seas.ucla.edu).

Publisher Item Identifier S 1063-6536(00)01412-3.

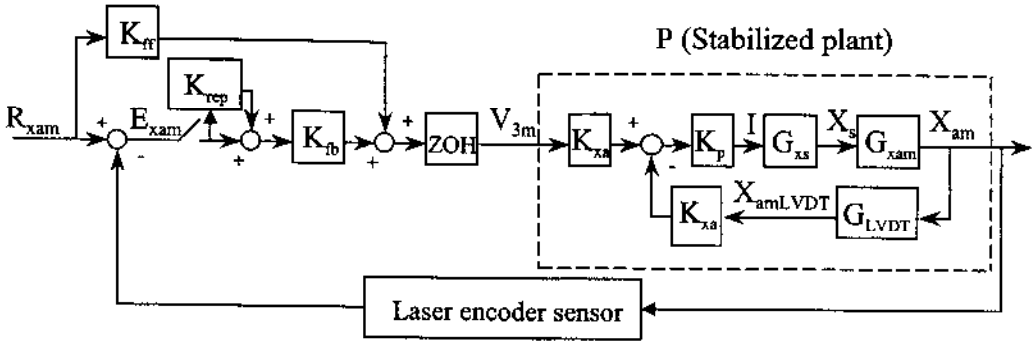

Fig. 1. Control system block diagram.

motions. For a less aggressive class of cam profiles, the data for a small range of magnitudes should be used to determine a nominal linear model, which minimizes frequency-wise its distance from all the included data points. The maximum distance is thus the uncertainty bound of the nominal model, which has been minimized to facilitate robust performance control design. For a more aggressive class of cam profiles, the nominal model should be determined from frequency response data that include a large range of magnitudes, and thus has a larger uncertainty bound. Of course, the tradeoff for including a larger range motion is reduced achievable robust performance due to the larger uncertainty bound.

The robust performance feedback controller alone cannot track periodic cam profile motions precisely due to its compromising nature to account for system nonlinearities as uncertainties. A feedforward tracking controller and a repetitive controller are designed based on the same nominal model used in the feedback controller design and implemented as plug-ins to the feedback controller. It will be shown that this controller structure has the feature that the sensitivity function is expressed as the multiplication of three terms that correspond to the individual effect of the three controllers separately.

The remainder of this paper is organized as follows. Section II describes the experimental system and presents the linear models and uncertainty bounds corresponding to different amplitude ranges of experimental frequency response data. Section III presents the robust performance feedback control design approach. Section IV presents some experimental results in terms of sensitivity functions and step responses for a range of input magnitudes. Section V describes the feedforward and repetitive plug-in controllers for electronic cam motion generation. Section VI presents the experimental results of the cam profile tracking and compares the performance of the various controllers for tracking cam profiles with different amplitudes, followed by the concluding remarks in Section VII.

II. System Description and Models

The experimental system consists of a flapper nozzle type two-stage servovalve, a double-ended equal-area linear displacement actuator, two displacement feedback sensors, and peripheral devices such as hydraulic power supply, valve drive servo amplifier, and digital signal processor board with host computer. The hydraulic system was operated at a supply pressure of 18.6 MPa (2700 lbf/in^2). The controllers were implemented on a 32-bit floating point digital signal processor (TMS320C30). As shown in the control system block diagram (Fig. 1) the hydraulic system is represented by two cascaded linear models, the servovalve model and the actuator model, where "$x_{\rm am}$" is the actuator position, "x_s" is the spool position, and "i" is the input current to the torque-motor. An analog proportional feedback loop (with gain $K_p = 1$ Volt/Volt), which is established by the servo amplifier electronics, creates a stabilized plant with input signal "v_{3m}," that has the same units as the actuator position "$x_{\rm am}$" (i.e., meters). This analog loop centers the actuator at the null position and is considered as the "open-loop" continuous-time plant in the digital control synthesis.

Two sensors are used for the actuator piston. First, a linear variable differential transducer (LVDT) is used for the analog proportional control loop, with an output range of ± 2.5 V for the full actuator stroke of ± 0.0254 m, i.e., $K_{xa} = 100$ V/m. Second, a laser-driven linear encoder with a resolution of 0.6 μm per count is used for the digital control feedback loop. The laser sensor dynamics are negligible and that is the reason for using it as the feedback sensor for precise cam profile tracking. The LVDT sensor dynamics was experimentally determined to have a bandwidth (using the -3 dB reduction criterion) of 800 Hz [9]

$$G_{\rm LVDT}(s) = \frac{x_{\rm amLVDT}(s)}{x_{\rm am}(s)} = \frac{2.82e^{11}}{s^3 + 1.40e^4 s^2 + 8.95e^7 s + 2.82e^{11}}. \quad (1)$$

The experimental frequency responses from the input "v_{3m}" to the LVDT output "$x_{\rm amLVDT}$" were measured with a signal analyzer, using a "swept-sine" method that generates fixed-amplitude sine waves of various frequencies, for input "v_{3m}" amplitudes of 0.5 mm, 1 mm, 2 mm, 3 mm, 4 mm, and 5 mm, respectively. The results in Fig. 2 clearly show system nonlinearities as the magnitude ratios are significantly different for different input amplitudes. Further examination of the servovalve and actuator frequency responses separately shows that the system nonlinearies are concentrated mostly in the servovalve [9].

Because the parameters for the servovalve nonlinear model are difficult to determine, the system is modeled with a number

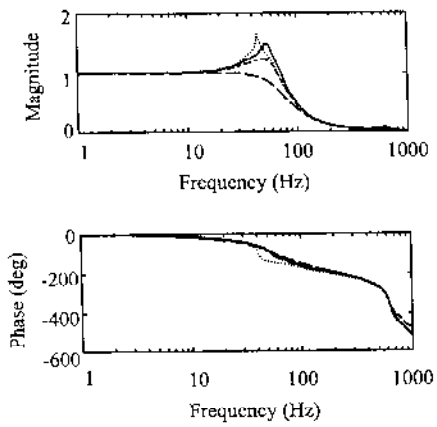

Fig. 2. Frequency responses of the plant: 0.5 mm input (dash), 2.0 mm input (dash-dot), 3.0 mm input (solid), 5.0 mm input (dot).

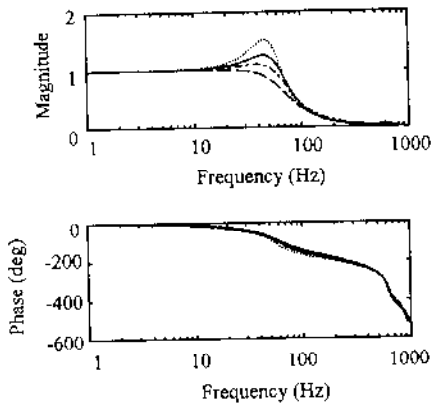

Fig. 3. Plant models for amplitude ranges 0.5 mm input (dash), 0.5 mm–2.0 mm input (dash-dot), 0.5 mm–3.0 mm input (solid), 0.5 mm–5.0 mm input (dot).

of linear models corresponding to increasing input amplitude ranges as shown below

Range A: Input $v_{3m} = 0.5$ mm
Range B: Input $v_{3m} = 0.5$ mm, 1 mm
Range C: Input $v_{3m} = 0.5$ mm, 1 mm, 2 mm
Range D: Input $v_{3m} = 0.5$ mm, 1 mm, 2 mm, 3 mm
Range E: Input $v_{3m} = 0.5$ mm, 1 mm, 2 mm, 3 mm, 4 mm
Range F: Input $v_{3m} = 0.5$ mm, 1 mm, 2 mm, 3 mm, 4 mm, 5 mm. (2)

In order to characterize the system dynamics completely within each range of motion, the chosen linear model must represent the best curve fit relative to all of the system frequency responses within that range. Therefore, for each range, a nominal frequency response $P_o(j\omega)$ and uncertainty bound $M(\omega)$ will be determined followed by a transfer function curve-fitting to determine the nominal linear model (transfer function) and uncertainty weighting filter.

Each set of frequency response data in a particular range can be represented by the following form:

$$P_i(j\omega) = [1 + M_i(j\omega)]P_o(j\omega). \tag{3}$$

Here, $P_o(j\omega)$ is the nominal frequency response to be determined and $M_i(j\omega)$ characterizes the size of the model uncertainty of the linear model with respect to the particular experimental curve. In order to facilitate the robust performance control design for each range, the linear model must be chosen such that the model uncertainty with respect to the pertinent experimental data is minimized. Thus the nominal frequency response $P_o(j\omega)$ is determined by minimizing the maximum uncertainty $M(j\omega)$ for each frequency, where

$$M(\omega) = \max_i |M_i(j\omega)|. \tag{4}$$

The nominal linear transfer function model then is obtained by curve fitting the nominal frequency response data using a particular eighth-order structure determined from physical modeling [8]. The linear nominal models shown in Fig. 3 exhibit the

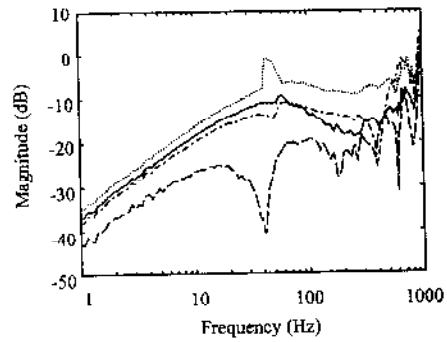

Fig. 4. Multiplicative uncertainty for amplitude ranges 0.5 mm input (dash), 0.5 mm–2.0 mm input (dash-dot), 0.5 mm–3.0 mm input (solid), 0.5 mm–5.0 mm input (dot).

similar characteristics to the experimental data, i.e., the larger input amplitude ranges correspond to larger magnitude peaks and sharper phase drops. Because the laser sensor output "x_{am}" is used for feedback controller design, the transfer function is further post multiplied by the inverse of the LVDT dynamics as in (1) to get the transfer function with that particular output.

Because there is additional model mismatch from the curve fitting process, the multiplicative uncertainty bound $M(\omega)$ is recalculated, which is shown in Fig. 4 for several ranges. The uncertainty progressively becomes larger as the model covers a larger range motion. The uncertainty data in the figure then are upper-bounded by a fixed-order filter $W_r(s)$ of the following form:

$$W_r(s) = \frac{n_0 s^2 + n_1 s + n_2}{s^2 + d_1 s + d_2}. \tag{5}$$

III. Robust Performance Control System Design

Controllers provide robust performance for a system if they maintain stability and achieve performance in the presence of model uncertainty. The main objective of the following controller design is to determine the achievable robust performance using the nominal plant models for the different amplitude ranges.

The theoretical background for the robust performance control system design is described next. The system dynamics are modeled with multiplicative uncertainty in the form of

$$P(s) = [1 + \Delta(s)W_r(s)]P_o(s) \tag{6}$$

where $P(s)$ represents experimental frequency response data, $P_o(s)$ is the nominal model, and $W_r(s)$ is a fixed stable transfer function which bounds the model uncertainty. The function $\Delta(s)$ is a variable stable transfer function satisfying

$$\|\Delta(s)\|_\infty := \sup_\omega |\Delta(j\omega)| \leq 1. \tag{7}$$

A necessary and sufficient condition for robust performance [10] is

$$\| |W_p S_o| + |W_r T_o| \|_\infty < 1 \tag{8}$$

where

$$S_o := \frac{1}{1 + P_o K_{\text{fb}}} \tag{9}$$

$$T_o := \frac{P_o K_{\text{fb}}}{1 + P_o K_{\text{fb}}} \tag{10}$$

and K_{fb} is the feedback controller shown in Fig. 1.

Typically, the performance weight $W_p(s)$ has larger magnitudes at lower frequencies, indicating desired tracking at these frequencies. An equivalent condition for robust performance is

$$\|W_p S\|_\infty < 1 \tag{11}$$

where

$$S := \frac{1}{1 + PK_{\text{fb}}} = \frac{e_{\text{zam}}}{r_{\text{zam}}}. \tag{12}$$

There is no known procedure to find directly the minimum achievable value of the norm of (8), and the corresponding controller $K_{\text{fb}}(s)$. A modified robust performance problem, known as the mixed sensitivity problem [11] can be applied, where the objective is to minimize

$$\sup_\omega \sqrt{|W_p(j\omega)S_o(j\omega)|^2 + |W_r(j\omega)T_o(j\omega)|^2}. \tag{13}$$

The mixed sensitivity problem is solved as a standard problem in the H^∞ framework [12].

The general procedure for the robust performance control system design is described next. The discrete nominal plants $P_o(z)$ are computed from the plant models, using a zero-order-hold transformation and then Tustin transformations are performed via the relation

$$z = \frac{1 + \frac{T}{2}w}{1 - \frac{T}{2}w} \tag{14}$$

where "T" is the sampling interval, resulting in plants $P_o(w)$. A sampling interval (T) of 0.5 ms is chosen, which is sufficient because the plant bandwidth $\approx$ 50 Hz for each input amplitude. The designs are performed in the w-domain because each controller $K_{\text{fb}}(w)$ can be mapped directly to the discrete controller $K_{\text{fb}}(z)$ without any approximation. The model uncertainty bounds $W_r(w)$ are obtained from (5), assuming a direct mapping from the s-domain to the w-domain. The performance weights are chosen to have the following low-pass form:

$$W_p(w) = \frac{K_{\text{wp}}}{\tau w + 1}. \tag{15}$$

TABLE I
RESULTS OF ROBUST PERFORMANCE CONTROLLER DESIGN

Input range	Limit break frequency (=1/τ) for Robust Performance Control Design	Maximum Allowable Reference Amplitude
A	0.167 rad/sec	0.4 mm
B	0.158 rad/sec	0.5 mm
C	0.149 rad/sec	0.7 mm
D	0.125 rad/sec	1.0 mm
E	0.1 rad/sec	1.5 mm
F	0.085 rad/sec	2.0 mm

IV. EXPERIMENTAL RESULTS OF ROBUST PERFORMANCE FEEDBACK CONTROL

Robust performance control design is performed for each range, using a fixed low-frequency magnitude ($K_{\text{wp}} = 3200$) for the performance weight (15) to ensure steady state performance. The break frequency is increased until the limit of the robust performance condition (8) is reached, and the results are provided in Table I. The limit break frequency of $W_p(w)$ is smaller for the larger ranges due to the increased model uncertainty. At the two extremes, the limit break frequency for the smallest range A is twice as large as the limit frequency for the largest range F.

The digital controllers obtained from converting the w-domain designs to the z-domain are implemented. The experimental sensitivity functions (12) of the sampled data system are obtained by using the signal analyzer "swept sine" method. The experimental sensitivity functions and the inverse of the W_p function corresponding to controller "A" and controller "F" are shown in Figs. 5 and 6, respectively. For controller "A" condition (11) is met for a reference amplitude of 0.15 mm, which implies that robust performance is achieved. In contrast, robust performance is not achieved for the 0.5 mm reference amplitude at frequencies near 100 Hz. For controller "F" condition (11) is met for reference amplitudes of 0.15 mm and 2.0 mm as shown in Fig. 6. The maximum reference amplitude for which robust performance is achieved using each controller is provided in Table I. The controllers designed from the linear models corresponding to the larger ranges provide robust performance for a wider range of reference amplitudes. This result validates the strategy to use linear models for different motion ranges.

The achieved performance with the robust performance controllers is analyzed further using the closed-loop step responses which are obtained for various reference amplitudes. The controllers designed from the larger ranges will provide similar closed-loop step responses for a wider range of reference amplitudes. The similarity of each step response is measured using the root mean square (RMS) difference between the normalized step response for that particular reference amplitude and the normalized step response for the smallest reference amplitude of

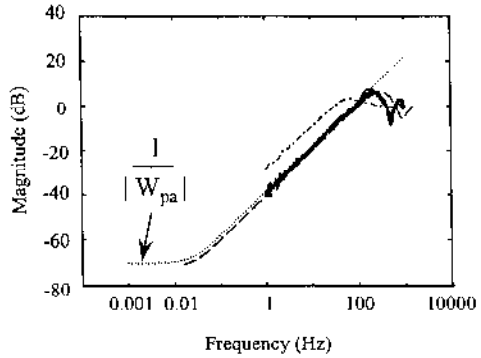

Fig. 5. Sensitivity functions using robust performance controller "A": open-loop plant data for 0.5-mm input (dash-dot), closed-loop nominal model prediction (dash), experimental data with reference = 0.15 mm (dark solid), experimental data with reference = 0.5 mm (solid).

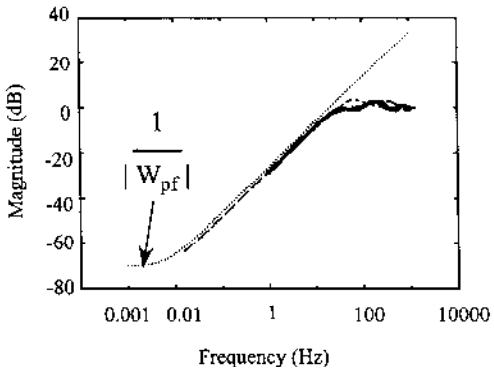

Fig. 6. Sensitivity functions using robust performance controller "F": open-loop plant data for 0.5-mm input (dash-dot), closed-loop nominal model prediction (dash), experimental data with reference = 0.15 mm (dark solid), experimental data with reference = 2.0 mm (solid).

0.1 mm. This particular rms index is a valid method of measuring the similarity of the normalized step responses, because it reflects discrepancies in rise time, overshoot, and overall step response.

The closed-loop step responses are similar for a wider range of reference amplitudes using the controllers designed from the models corresponding to the larger ranges, as confirmed by the data in Table II. The normalized step responses using the controller "A," shown in Fig. 7, demonstrate that the step response for the smallest reference amplitude (0.1 mm) is very similar to the model prediction, while the response for the larger reference (1.5 mm) is very different from the predicted response. The step responses using the controllers designed from the smaller ranges (A, B, C) are even unstable for the reference amplitudes which are beyond the range of the experimental data used to determine the particular nominal model.

V. Repetitive and Feedforward Controllers

The tracking performance by the robust performance feedback controllers presented above is not satisfactory for precise cam profile generation because of the dynamic delays in the closed-loop system characterized by the sensitivity function in (9). It is noted here that one degree phase mismatch of a single harmonic wave will generate about 1.7% maximum tracking error in magnitude. Repetitive control and feedforward control are used in a plug-in manner as shown in Fig. 1 to achieve superior tracking performance.

The discrete-time repetitive controller as described in [1] and [2] is designed based on the nominal closed-loop return difference $T_o(z^{-1})$ in (10)

$$T_o(z^{-1}) = \frac{z^{-d}B_{\rm cl}(z^{-1})}{A_{\rm cl}(z^{-1})} \tag{16}$$

$$A_{\rm cl}(z^{-1}) = 1 - a_1 z^{-1} - \cdots - a_n z^{-n}$$
$$B_{\rm cl}(z^{-1}) = b_0 + b_1 z^{-1} + \cdots + b_m z^{-m}, \quad b_0 \neq 0.$$

The repetitive controller is

$$K_{\rm rep}(z^{-1}) = \frac{M(z^{-1})Q(z,z^{-1})z^{-N}}{1 - Q(z,z^{-1})z^{-N}} \tag{17}$$

$$M(z^{-1}) = \frac{A_{\rm cl}(z^{-1})B_{\rm cl}^{-}(z)z^{d}}{B_{\rm cl}^{+}(z^{-1})b}$$
$$b = (|b_0| + |b_1| + \cdots + |b_m|)^2.$$

Here, N represents the number of data points in one cycle, $B_{\rm cl}^{+}(z^{-1})$ contains the zeros of $B_{\rm cl}(z^{-1})$ to be cancelled, and $B_{\rm cl}^{-}(z^{-1})$ must contain all the roots of $B_{\rm cl}(z^{-1})$ outside or on the unit circle to avoid unstable pole-zero cancellation. Also, $B_{\rm cl}^{-}(z)$ is obtained by substituting z for z^{-1} in $B_{\rm cl}^{-}(z^{-1})$. In this paper, the repetitive controllers are formed by assuming $B_{\rm cl}^{-}(z^{-1}) = B_{\rm cl}(z^{-1})$ and $B_{\rm cl}^{+}(z^{-1}) = 1$. This ensures that the repetitive controller will be a finite impulse response filter.

The low-pass, zero-phase filter $Q(z,z^{-1})$ is included to guarantee robust stability for the repetitive controller. For this, the multiplicative uncertainty bound for the closed-loop return difference T_o is calculated in the discrete-time domain from the open-loop bound $M(\omega)$ for each case and denoted as $M_{\rm cl}(\omega)$. The following robust stability condition can be derived [2] to determine Q:

$$Q(\omega) < \frac{1}{M_{\rm cl}(\omega)}. \tag{18}$$

The results are $Q(z,z^{-1}) = [0.1z\ 0.8\ 0.1z^{-1}]$ for range "F" and $Q = 1$ for other smaller ranges.

The feedforward controller implements the zero phase error tracking controller (ZPETC) [13] based on the open-loop nominal plant model $P_o(z^{-1})$

$$P_o(z^{-1}) = \frac{z^{-d}B(z^{-1})}{A(z^{-1})} \tag{19}$$

$$K_{\rm ff}(z^{-1}) = \frac{z^{d}A(z^{-1})B^{-}(z)}{B^{+}(z^{-1})[B^{-}(1)]^2} \tag{20}$$

where $B^{-}(z)$ and $B^{+}(z^{-1})$ are as previously described.

The tracking performance characterized by the sensitivity function for the nominal plant model is

$$S_{\rm nom} = S_o(1 - P_o K_{\rm ff})\frac{1 - Qz^{-N}}{1 + Q(MT_o - 1)z^{-N}}. \tag{21}$$

It is easy to see the multiplying effect of adding the plug-in feedforward and the repetitive controllers to the feedback controller.

TABLE II
RMS DIFFERENCES FROM NORMALIZED STEP RESPONSES WITH ROBUST PERFORMANCE CONTROLLERS

Reference amplitude	Control A	Control B	Control C	Control D	Control E	Control F
0.3 mm	0.04	0.04	0.04	0.03	0.04	0.03
0.5 mm	0.07	0.05	0.05	0.04	0.04	0.03
0.75 mm	0.12	0.10	0.10	0.06	0.06	0.03
1.0 mm	0.17	0.14	0.13	0.09	0.11	0.03
1.5 mm	0.20	0.18	0.15	0.13	0.12	0.05
2.0 mm	0.45	0.35	0.34	0.15	0.14	0.06
2.5 mm	0.53	0.35	0.35	0.27	0.25	0.06
3.0 mm	Unstable	0.48	0.41	0.27	0.25	0.08
3.5 mm	Unstable	Unstable	0.42	0.28	0.26	0.09
4.0 mm	Unstable	Unstable	Unstable	0.30	0.28	0.10

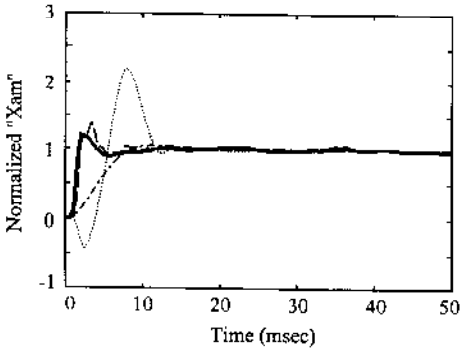

Fig. 7. Normalized step responses using robust performance controller "A": open-loop plant data for 0.5-mm input (dash-dot), closed-loop nominal model prediction (dash), experimental data with reference = 0.1 mm (dark solid), experimental data with reference = 1.5 mm (dot).

VI. EXPERIMENTAL RESULTS FOR CAM PROFILE TRACKING

The reference trajectory corresponding to electronic cam motion is shown in Fig. 8, with 9.4 mm maximum displacement, 1.2 m/s maximum speed, and 1000 m/s^2 maximum acceleration. This cam trajectory contains 200 points (i.e., $N = 200$) and for the equivalent spindle speed of 600 r/min, the reference frequency is 10 Hz and the sampling frequency is 2000 Hz. Three performance indices are used to quantify the results. The accuracy of the cam tracking performance is characterized by the maximum error and RMS error. The consistency of the cam tracking performance, i.e., the cycle-to-cycle variation, is characterized using the rms difference between the particular error response and the averaged error response over a number of cycles. In the experimental results presented below, five cycles of tracking error data were collected for each case evaluated. The numbers presented are the averaged values obtained from each of the five cycles.

Initially, the pure repetitive control strategy of Tsao and Tomizuka [1], [2] is used: a discrete-time repetitive controller is designed from the stabilized open-loop plant model corresponding to the smallest amplitude range A. The implementation of this controller achieves performance of 75 μm maximum error, 17.5-μm rms error, and 15.2-μm rms cycle-to-cycle variation, each value being the average for five cycles. The error responses for two cycles shown in Fig. 9 demonstrate that this controller does not provide adequate tracking of the periodic cam trajectory, especially because of the large rms cycle-to-cycle variation caused by an alternating cycle pattern.

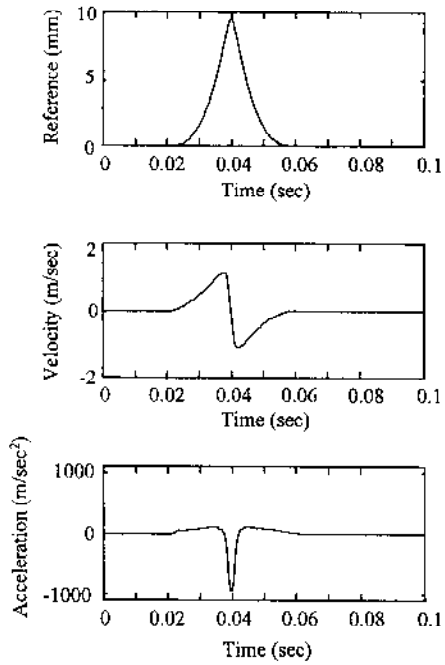

Fig. 8. Reference trajectory with velocity and acceleration profiles.

A model corresponding to a larger range of actuator motion is needed to provide better tracking performance for this reference cam trajectory, specifically the model corresponding to the largest amplitude range F. To validate the point that the range of required motion determines the appropriate model and controller, the controllers designed from each of the six models were implemented to track the reference trajectory of Fig. 8 scaled to five different degrees: full scale, three-quarter scale, half scale, three-tenth scale, and one-tenth scale. These five scaling levels correspond to peak reference amplitudes of 9.4 mm, 7.1 mm, 4.8 mm, 2.9 mm, and 1.0 mm, respectively. As indicated in Fig. 1, the robust performance controller for each model is implemented with two other controllers: the repetitive controller designed from the closed-loop model with this robust performance controller, and the zero phase error feedforward controller designed from the plant model P_o. The model and controller parameters are not presented here but the details can be found in [9]. The experimental results in terms of the three performance indexes are shown in Table III. In each experimental run, five cycles of tracking error data were recorded

TABLE III
EXPERIMENTAL RESULTS OF CAM PROFILE TRACKING (UNITS: μm)

Tabulated Data: Max Error (std.dev.) RMS Error (std.dev.) Cycle-to-Cycle Variation (std.dev.)	Control A	Control B	Control C	Control D	Control E	Control F
1/10 scale reference trajectory	10 (2) 4.1 (0.7) 4.1 (0.6)	12 (2) 4.4 (0.6) 4.3 (0.7)	12 (1) 4.6 (0.6) 4.0 (0.7)	13 (2) 5.1 (0.5) 3.8 (0.6)	11 (2) 5.2 (0.5) 3.4 (0.6)	12 (2) 5.1 (0.6) 3.3 (0.5)
3/10 scale reference trajectory	12 (2) 4.1 (0.6) 3.9 (0.4)	12 (2) 4.4 (0.6) 4.1 (0.5)	13 (3) 5.2 (0.6) 4.4 (0.6)	12 (3) 5.3 (0.5) 4.6 (0.6)	15 (3) 5.6 (0.8) 3.5 (0.5)	16 (2) 7.1 (0.8) 4.0 (0.5)
1/2 scale reference trajectory	16 (4) 6.0 (0.6) 5.9 (0.5)	17 (4) 6.4 (0.4) 5.8 (0.4)	16 (3) 6.4 (0.4) 4.9 (0.5)	11 (2) 4.8 (0.4) 4.2 (0.5)	15 (3) 5.9 (0.5) 4.3 (0.4)	22 (2) 7.8 (0.5) 3.9 (0.4)
3/4 scale reference trajectory	31 (8) 7.1 (1.1) 6.9 (0.8)	29 (8) 7.4 (0.9) 6.7 (0.9)	24 (7) 7.1 (1.0) 7.1 (0.8)	16 (4) 4.1 (0.5) 6.5 (0.6)	11 (3) 5.0 (0.6) 4.1 (0.3)	25 (4) 5.7 (0.6) 3.8 (0.3)
Full scale reference trajectory	73 (11) 17.0(2.1) 14.8 (2.9)	75 (9) 15.9 (2.1) 12.7 (2.6)	63 (9) 11.6 (2.3) 9.6 (2.7)	44 (6) 9.3 (0.8) 6.7 (1.3)	23 (3) 7.3 (0.7) 5.1 (0.7)	26 (4) 6.8 (0.5) 4.6 (0.7)

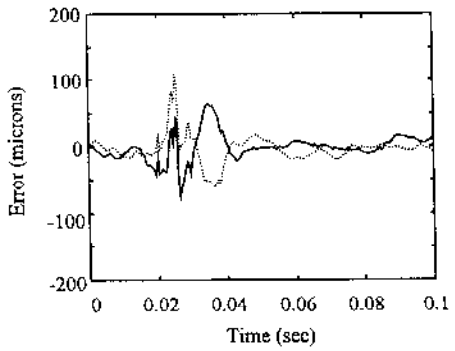

Fig. 9. Error responses with only repetitive control: Cycle 1 (solid), Cycle 2 (dot).

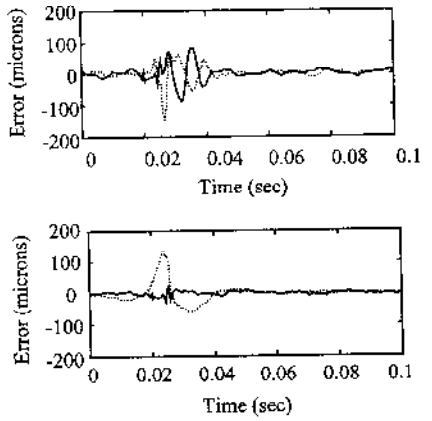

Fig. 10. Tracking errors for full scale reference trajectory.Top (Case A): H^∞ feedback control with repetitive control (dot), H^∞ feedback control with repetitive control and feedforward control (solid). Bottom (Case F): H^∞ feedback control with repetitive control (dot), H^∞ feedback control with repetitive control and feedforward control (solid).

after the control system reached its steady state. The maximum error and rms error were calculated for each of the five cycles. For the cycle-to-cycle variations, an averaged one-cycle error profile was first calculated from the five-cycle data, and then the rms deviations of each cycle from this averaged profile were calculated. The values shown in Table III are the averaged values over the five cycles and the values in the parentheses are the standard deviations of the five numbers from their average.

By comparing all three indexes for each controller at different levels of cam profile magnitude, it can be judged that controllers "A" and "B" achieve the best performance for the one-tenth and three-tenth scale. Similarly, controller "D" for the one-half scale, controller "E" for the three-quarters scale, and controller "F" for the full scale of the reference profile, respectively, can be concluded. For small motion like the one-tenth scale reference, it is not beneficial to use controllers from larger amplitude ranges since their feedback performances are poorer. The maximum tracking error for the full scale profile using controller "F" is about 0.28% of the profile magnitude, indicating a precise synchronization between the master and the slave axis. As expected, the tracking results for the full scale trajectory become progressively worse as the model amplitude range decreases, as the worst performance is obtained using the controller "A," which is designed from the model corresponding to the smallest motion range A. The error responses for these two cases are shown in Fig. 10, in addition to the error responses with just robust performance feedback control and repetitive control. The inclusion of the feedforward controller improves the tracking results in case F. On the other hand, the tracking performance would also be poor (not shown in the figure) if only the feedforward controller were included without the repetitive controller. This suggests the synergistic effect of all three controllers acting together to achieve superior performance.

VII. CONCLUSION

An effective strategy for modeling and control design has been developed for the electrohydraulic actuator to generate

electronic cam motion. The nonlinear dynamics are represented by a number of linear models with associated bounds of model uncertainty. For each specified range of motion trajectories, a robust performance controller is designed from the particular linear model and corresponding uncertainty bound to ensure consistent performance under the effect of nonlinear dynamics in that range. The experimental sensitivity functions and step responses demonstrate that the controllers designed from the larger range models provide robust performance for a wider range of reference signals. To precisely generate electronic cam motion for reference trajectories of different amplitudes, a repetitive controller and a feedforward controller are added as plug-ins to the feedback controller. The experimental tracking results confirm that as the maximum amplitude of the reference trajectory increases, the best tracking performance is obtained using the controllers designed from the model corresponding to a larger range of actuator motion. Conceptually, this approach can be utilized to generate a number of controllers corresponding to a progressively increased level of motion aggressiveness. One can then select the best among the suite of controllers according to the particular motion application at hand and switch from one to another as the application demands change. The method proposed in this paper has also been applied to a similar type of electrohydraulic actuator for the actual noncircular machining operation and achieved similar results reported here [14].

REFERENCES

[1] T.-C. Tsao and M. Tomizuka, "Adaptive and repetitive digital control for noncircular machining," in *Proc. Amer. Contr. Conf.*, 1988, pp. 115–120.

[2] — —, "Robust adaptive and repetitive digital tracking control and application to a hydraulic servo for noncircular machining," *ASME J. Dynamic Syst., Measurement, Contr.*, vol. 116, pp. 24–32, 1994.

[3] N. Hori, A. S. Pannala, P. R. Ukrainetz, and P. N. Nikiforuk, "Design of an electrohydraulic positioning system using a novel model reference control scheme," *ASME J. Dynamic Syst., Measurement, Contr.*, vol. 111, pp. 294–295, 1989.

[4] S. R. Lee and K. Srinivasan, "Self-tuning control application to closed-loop servohydraulic material testing," *ASME J. Dynamic Syst., Measurement, Contr.*, vol. 112, pp. 682–683, 1990.

[5] A. Akers and S. J. Lin, "Optimal control theory applied to a pump with single-stage electrohydraulic servovalve," *ASME J. Dynamic Syst., Measurement, Contr.*, vol. 110, pp. 121–127, 1988.

[6] Z. Shichang, C. Xingmin, and C. Yuwan, "Optimal control of speed conversion of a valve controlled cylinder system," *ASME J. Dynamic Syst., Measurement, Contr.*, vol. 113, p. 693, 1991.

[7] H. E. Merritt, *Hydraulic Control Systems*. New York: Wiley, 1967, pp. 147–150, 312–318.

[8] D. Kim and T. C. Tsao, "An improved linearized model of electrohydraulic servovalves and its usage for robust performance control system design," in *Proc. Amer. Contr. Conf.*, June 1997, pp. 3807–3808.

[9] D. H. Kim, "Precision Motion Control of Electrohydraulic Actuators," Ph.D. dissertation, Dept. Mechanical Ind. Eng., Univ. Illinois, 1997.

[10] J. Doyle, "Analysis of feedback systems with structured uncertainties," *Proc. Inst. Elect. Eng.*, pt. D, vol. 129, pp. 242–250, 1982.

[11] H. Kwakernaak, "Minimax frequency domain performance and robustness optimization of linear feedback systems," *IEEE Trans. Automat. Contr.*, vol. AC-30, no. 10, pp. 994–1004, 1985.

[12] B. A. Francis, *A Course in H^∞ Control Theory*. Berlin, Germany: Springer-Verlag, 1987, pp. 15–22, 75–83.

[13] M. Tomizuka, "Zero phase error tracking algorithm for digital control," *ASME J. Dynamic Syst., Measurement, Contr.*, vol. 109, pp. 65–68, 1987.

[14] T.-C. Tsao, R. D. Hanson, T. Sun, and A. Babinski, "Motion control of noncircular turning process for camshaft machining," in *Proc. Japan-USA Symp. Flexible Automation*, Otsu, Japan, 1998, pp. 485–489.

Dean H. Kim received the B.S. degree from Cornell University, Ithaca, NY, in 1989, and the M.S. and Ph.D. degrees from the University of Illinois, Urbana-Champaign, in 1993 and 1997, respectively, all in mechanical engineering.

He is currently an Assistant Professor in the Department of Mechanical Engineering at Bradley University in Peoria, IL. His research interests include dynamic modeling and applied controls for mechanical systems, such as hydraulic actuators, engines, and fluid systems. He also has supervised student projects in these areas with Caterpillar and with the John Deere Corporation.

Dr. Kim is a Member of ASME.

Tsu-Chin Tsao (S'86–M'88) received the B.S. degree from National Taiwan University in 1981 and the M.S. and Ph.D. degrees from the University of California, Berkeley, in 1984 and 1988, all in mechanical engineering.

He was an Associate Professor at University of Illinois at Urbana-Champaign (UIUC), before joining University of California, Los Angeles, in 1999. His research interests include dynamic modeling and control of mechanical systems, manufacturing processes, and automotive systems.

Dr. Tsao is a Member of ASME and a Senior Member of SME. His research has been recognized by the 1994 Best Paper Award of ASME Journal of Dynamic Systems, Measurement, and Control, UIUC College of Engineering Xerox Award for Faculty Research in 1996, and ASME Dynamic Systems and Control Outstanding Young Investigator Award in 1997.